

# SEMI AUTOMATED IMPROVEMENT OF WIND BLADE DESIGN

*D. Perfiliev - A. Kosmacheva – J. Backman – J. Hämäläinen*

Laboratory of Fluid Dynamics, LUT Energy, Lappeenranta University of Technology,  
Lappeenranta, Finland, daniil.perfiliev@lut.fi, jari.backman@lut.fi

Centre of Computational Engineering and Integrated Design, Lappeenranta University of  
Technology, Lappeenranta, Finland, anna.kosmacheva@lut.fi, jari.hamalainen@lut.fi

## ABSTRACT

**This work develops an iterative semi-automated mechanism for wind blade geometry improvement. Implementation of the lately introduced aerodynamic, economic and mechanic analysis technique coupled with robust airfoil characteristics coding allowed to fasten the search procedure and to use the extensively applied Matlab programming environment. The obtained optimal solutions based on the power efficiency improvement while maintaining the same capital investments as the original blade geometry provided significant advantages.**

**While looking for the optimal chord and twist distribution for the considered WindPACT 1.5 MW wind turbine and IIB IEC wind class with the BEM approach, the power efficiency improved by 1.4% compared to the original blade geometry. The same procedure coupled with the optimal cross-sectional search provided an improvement of 4.9% in the power coefficient. The results were validated against the CFD-RANS procedure. With some minor fluctuations, the results of BEM and CFD agree well with each other.**

## Nomenclature

$b$	fixed part of the cost	$\delta$	unidirectional layer thickness
$Cl$	lift coefficient	$\omega$	specific dissipation rate
$Cd$	drag coefficient		
$C_p$	aerodynamic power coefficient		
$C_{rotor}$	rotor cost		
$c$	average blade element chord		
$L$	static blade-tower clearance		
$k$	turbulence kinetic energy		
$r$	radial blade distance		
$S$	blade element surface area		
$U$	wind speed		
$w_{rotor}$	weight parameter		
$\beta$	pitch angle		
$\lambda$	tip speed ratio		

## Subscripts and Superscripts

BEM	Blade Element Momentum
CFD	Computational Fluid Dynamics
HAWT	Horizontal Axis Wind Turbine
RANS	Reynolds Averaged Navier-Stokes
SMRF	Single Moving Reference Frame
$i$	considered blade shape on $i$ -th iteration
$j$	iterative variable
$orig$	original blade
$r.u.$	relative units

## INTRODUCTION

The global wind industry growth of more than 20% in 2011 and the average growth of 28% over the past decade (Evans, 2012) show the clear demand for fast and competitive tools for the analysis and design of wind turbines. From this perspective, developing tools for the optimization and improvement of wind turbine blade geometry can be seen as one of the most crucial tasks to solve. Many publications have been devoted to this problem. The authors have concentrated on different optimization factors, trying to maximize the power efficiency or minimize the overall budget. Fuglsang and Madsen (1999) presented an optimization method which allows multiple constraints and is objected for the minimum cost of energy which is determined by the given fatigue and extreme loads, as well as the annual energy production. Casas, Pena and Duro (2006) developed

a tool which searches for the blade shape with the maximum power efficiency by the means of macroevolutionary algorithms. Its aerodynamic analysis is based on a neural network simulator. In general, these methods lead to a situation where the turbine power improvement is achieved with a simultaneous budget increase. The optimization task is reduced to decide the compromise variant. In contrary to these approaches, we are looking for a method to achieve better performance results, i.e. in the power efficiency, however not affecting the cost function.

There are industrial applications for optimization based on computational fluid dynamics (CFD), e.g. for heat exchangers and paper production (Lyytikäinen, et al., (2009), Toivanen, et al. (2003)), but they are based on two-dimensional flow models which is a significant simplification. Sophisticated CFD procedures still cannot be widely applied in the optimization tasks despite the rapid growth of computational capacities. However, CFD simulation is used for the analysis of wind turbine flow characteristics that cannot be taken into account with classical blade element (BEM) or potential flow methods. It is very natural to check the final result of the BEM calculations with CFD to validate the design and to see whether, for example, there are unwanted areas of separation. Rajendran (2011) studied the Horizontal Axis Wind Turbine (HAWT) with numerically solved fluid dynamics equations. The research showed that the method works well and provides an adequate aerodynamic analysis. The effects of modifying the inboard portion of the NREL Phase VI rotor using a thickened, flat back version of the S809 design airfoil were considered by Chao and van Dam (2008). The results of this study demonstrate that a thick, flat back blade profile is viable as a bridge to connect structural requirements with aerodynamic performance when designing future wind turbine rotors.

We applied simplified engineer methods for the analysis, improvement search and decision making. Recently developed theories for aerodynamic, economic and mechanic investigation are used in this article. When the improvement task is solved with fast and robust tools, the results are validated against a more complicated CFD procedure by analyzing only several shapes, and on this basis, the applicability of the proposed improvement approach is proved. Based on works of Vermeer (2003), Hansen (2006), and Carcangiu (2008), which analyzed different CFD approaches and methods, the validation is made by simulating the wind blade performance with RANS equations and  $k-\omega$  SST turbulence model.

Starting with a general overview of the analysis tools and blocks, the article proceeds with the consideration of practical blade shape improvement based on a prototyped WindPACT 1.5 MW wind turbine blade. For the validation of the results, the explanation of the conducted CFD analysis is then presented in the following chapters. The article is closed with the result discussions and conclusions.

## GENERAL OVERVIEW OF ANALYSIS TOOLS

To have a general understanding of the improvement search procedure, the main analysis blocks are described first. The program blocks are written in Matlab environment as it is nowadays the most commonly used scientific programming language. The structure of the blocks and their connections are presented in Figure 1.

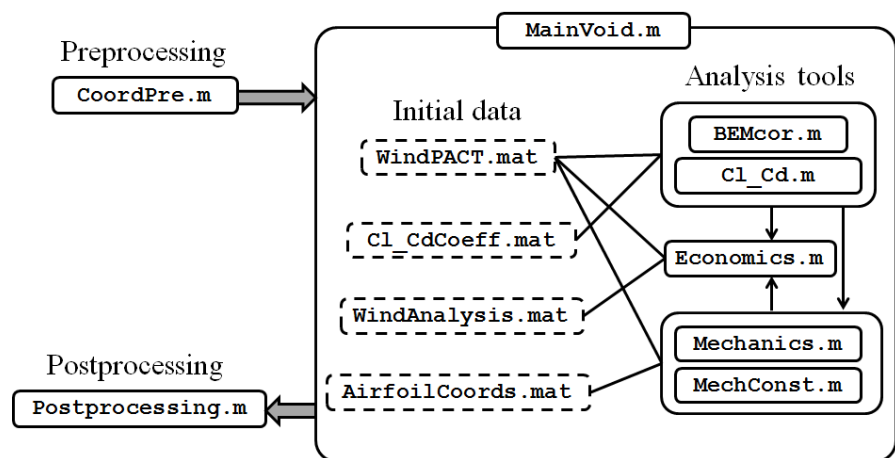


Figure 1. Structure of m-files

## Aerodynamics

The blade element moment theory is used in the aerodynamic block to calculate the flow angles of attack, lift and drag forces, moments, and power efficiency. Classical BEM built on an iterative procedure to calculate induction factors as described by Ingram (2011) and Moriarty and Hansen (2005) is expanded with corrections presented by Madsen et.al (2010) which account for the pressure variation from wake rotation and decrease the inflow at the blade tip due to the wake expansion. The procedure is conducted for design conditions, as well as extreme wind. For the design case, the following constant parameters are taken: tip speed ratio,  $\lambda$ , 6.9; pitch angle,  $\beta$ , 2 deg; wind speed,  $U$ , 7.5 m/s (corresponding to IIIB IEC wind turbine class). The values for tip speed ratio and pitch angle are derived from the modeling experiment with the original blade shape and intent to reach the maximum aerodynamic efficiency. The 50-year extreme wind speed according to IEC standard (IEC 61400-12-1, 2005) is five times greater than the yearly averaged one that is found from the Weibull distribution parameters of the actual construction location.

### Cl-Cd curves coding

Each cross-sectional airfoil is characterized by the experimental curves showing lift and drag coefficients for the corresponding flow angle of attack. These parameters can be presented graphically (usually) or tabulated. Merz (2011) developed an approach in which the airfoil characteristics are presented shortly with only several tabulated numbers. The intermediate values are calculated with the corresponding equations depending on the angle of attack. It decreases the database volume and fastens the procedure. However, the manually defined, and hence semi accurate, parameters taken from tables or graphs are a source of uncertainty in the overall procedure and may cause deviation from the practically observed results.

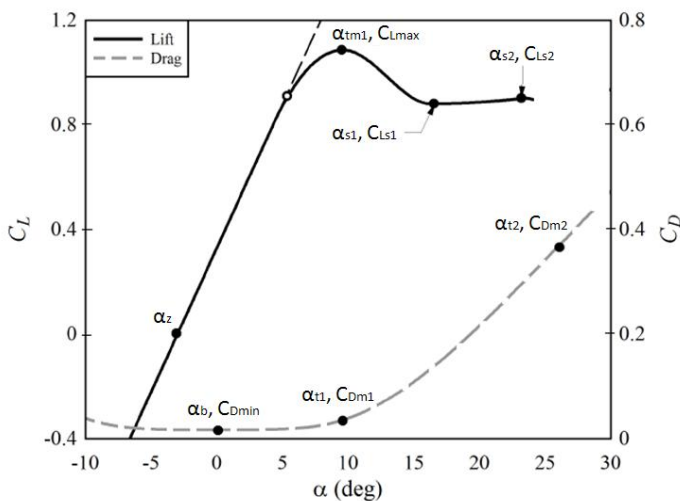


**Figure 2. Lift and drag curves coding, based on Merz (2011)**

Generally requested parameters are presented in Figure 2. For each profile, the designer has to provide only thirteen values (seven for the lift curve and six for the drag) of attack angles and the respective lift and drag coefficients. For the wind turbine case, we suspect that the Reynolds number does not play an important role, and its effect on the lift and drag curves can be neglected.

There are four regions on the lift curve and two on the drag one. These regions are described with linear or third order polynomial functions. More details on airfoil curves coding are presented by Merz (Merz, 2011).

## Mechanics

To prevent unrealistic design variants, the mechanical investigation is performed. The assumed structural layout of the blade consisting of composite materials is presented in Figure 3. The blade interior has three sections with two webs. The highly curved and short length leading edge part of the blade is assumed to stay buckle free, and is thus not considered in the mechanical analysis. The blade outer skin is covered with gelcoat, nexus and double-bias laminate composite materials. The laminate is defined as a stack of plies while a ply is a unit thickness composite material. However, the gelcoat and nexus layers are not taken into account in the mechanical investigation, as they do not contribute much to the structural stiffness. The gelcoat layer smoothes the blade surface, while soft nexus material provides a relatively smooth but absorbent surface for the gelcoat. The function of the double-bias laminate is to introduce shear strength and to prevent the splaying of the

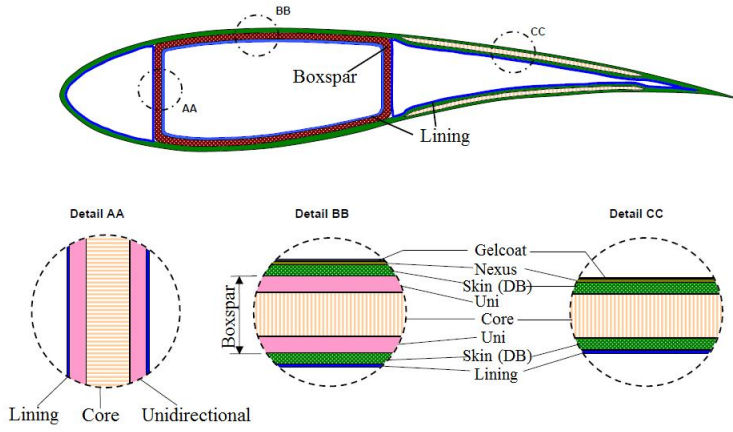


**Figure 3. Structural layout of composite blade. Based on Bir and Migliore (2004)**

is aimed to be improved with an additional possibility to choose several spar configurations, e.g. the blade to have a D-spar web configuration.

The mechanical procedure analyses the forces' and moments' act on the blade, and iteratively calculates the thickness of the unidirectional material needed for every cross-section to withstand three criteria: the tip deflection shall not be more than two thirds of the blade-tower clearance (Tong, 2010) and the blade has to fulfill the ultimate strength and buckling criteria (Bir and Migliore, 2004). The blade-tower clearance for the considered case of WindPACT 1.5 MW turbine is  $L=3.3\text{m}$  (Malcolm et al., 2002). Lining, double-bias and core material thicknesses are found with the trend equations based on the data from Bir and Migliore (2004) where calculations were made for a wind turbine of the same range. Structural properties of the blade like the axial stiffness and offset of the elastic axis are processed based on the considered blade geometry. The further details for governing equations and iterative procedure are given in the work of Bir and Migliore (2004)

### Economics

It is crucial to be confident that the wind turbine performs effectively, but also without demanding huge relative expenses. Hence, during the optimization procedure, various blade shapes are compared on the economic basis. The comparison is non-dimensional and deals with the relative costs of rotor production. The approach calculates the rotor cost,  $C_{rotor}$ :

$$C_{rotor} = b + (1 - b) * w_{rotor} \quad (1)$$

where  $b=0.1$  stays for the fixed parts of transportation and manufacturing costs, based on Xudong (2009) and  $w_{rotor}$  is the weight parameter that binds the original and considered blade geometries. It is calculated as:

$$w_{rotor} = \sum \frac{S_i \delta_i c_i}{S_{orig} \delta_{orig} c_{orig}} \quad (2)$$

where  $S$  is the blade element surface area,  $\delta$  the unidirectional layer thickness, and  $c$  the average chord of the blade element. The layer thicknesses of the unidirectional material are found at the mechanical analysis stage. The surface areas are found with known unit perimeters, chords and radial distances. More details are presented by Perfiliev (2011).

### PARAMETERS VARIATION USED FOR SEARCH PROCEDURE

Various blade outer geometries are shaped with changes in the chord, twist and cross-sectional distribution. Iteratively obtained shapes are then processed with the analysis tools. Hence, it is possible to cover blade geometries close within a certain range to the original one. From the

unidirectional material. The unidirectional material provides flexural and bending strength due to its load-bearing capabilities. The lining is usually presented with a double-bias layer and it covers the inside surface of the cells. All parts of the blade cross-section contain core material that serves for buckling strength.

The given unit coordinates of the airfoils are preprocessed to form a continuous line with the inserted lines of structural webs on 12% and 50% of the chord, according to Bir and Migliore (2004). Later on, the analysis

economic analysis perspective, it is advantageous that various considered blade shapes have the same distribution trend as the initial one, as it is assumed that the blade manufacturing process does not have to change radically. Instead, minor chord, twist and cross-sectional adjustments shall improve the overall performance of the blade used in certain wind conditions without significant changes in the production process.

### Chord variation

The initial chord distribution on the working part of the WindPACT 1.5 MW turbine blade considered in this article is close to linear, and hence, it was decided to model various chord distributions with the linear equation  $c=a \cdot r+b$ , where  $r$  stays for the radial blade distance,  $c$  for the local chord,  $a$  and  $b$  are defining parameters. The cross sections outside the working part, i.e. closer to the blade root, are neglected and not analyzed for the convenience of computation, and on the basis that this part does not contribute much to the overall rotor torque.

For the iterative procedure we introduce variable parameters  $dc$  (the overall interval of chord change),  $dc_1$  (the change in chord of ‘root’ cross section), and  $dc_2$  (the change in chord of ‘tip’ cross section). The visualized family of chord distributions is presented in Figure 5.

Within these abbreviations, the defining parameters of the linearly distributed chord equation for a certain  $i$ -th case of the loop are defined as:

$$a_i = \frac{c_0(1+2dc-dc_{1i}-dc_{2i})-c_{end}}{r_0-r_{end}} \quad (3)$$

$$b_i = c_0(1 + dc - dc_{1i}) - a_i r_0 \quad (4)$$

where  $c_0$  and  $r_0$  stay for the first chord and the first span of the initial blade geometry.

The blade designer has the ability to experiment with loop parameters  $dc_1$  and  $dc_2$  that change iteratively. For this article, we define them to vary in the range  $[0; 2*dc]$  with a step  $ddc=0.1*dc$ , where  $dc$  is assumed equal to 15% of the ‘root’ cross section.

### Twist variation

The radial twist distribution has a more sophisticated form than the chord one. Hence, it is not suitable to use exactly the same ‘linear’ approach. We present the initial blade twist distribution with function  $f_1(r)$ , and introduce a linear adjustment  $a_{twj}(r-r_0)+b_{twj}$  for each of its values. Function  $f_2(r)=f_1(r)+a_{twj}(r-r_0)+b_{twj}$  then describes the family of the blade twist distributions. Figure 6 presents that family graphically. In fact, this is not the only way to describe variable twist

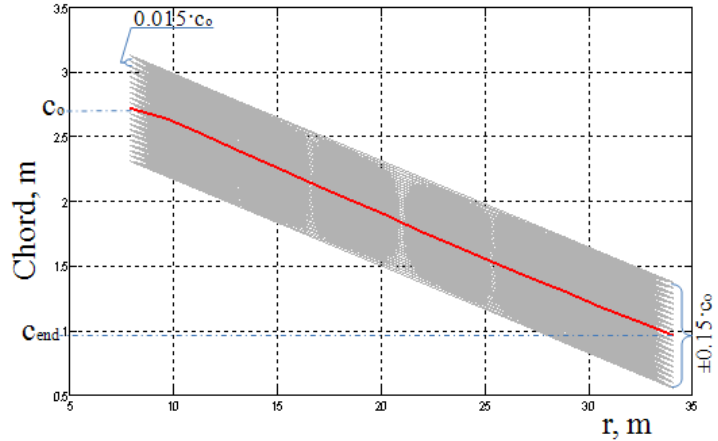


Figure 5. Considered chord distributions (colored line for original chord distribution).

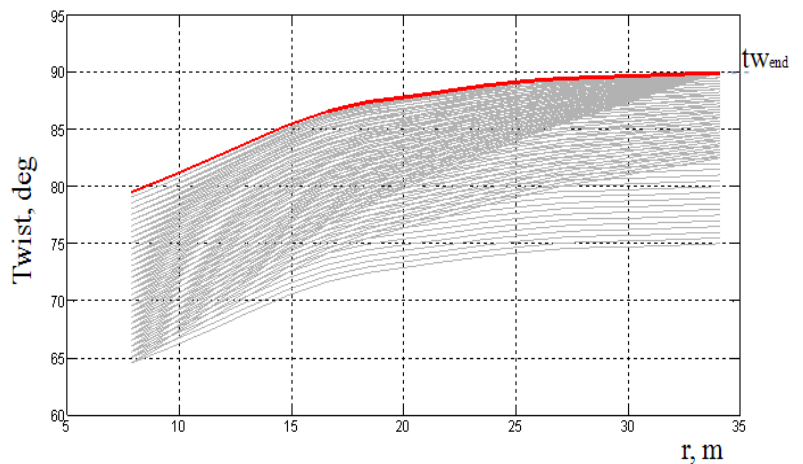


Figure 6. Considered twist distributions.

distributions, and we agree that it is far from the full solution, i.e. the equation does not provide the equal density for distributions within the family, but the article introduces this method on the basis of its simplicity and convenience for the particular case.

Defining parameters  $a_{twi}$  and  $b_{twi}$  are changed iteratively within the loop. The designer may experiment with its ranges. For this article, the value of  $b_{twi}$  changes from  $b_{down}=-15^\circ$  to  $b_{up}=90-tw_{end}$ ; the twist angle cannot be shaped for more than  $90^\circ$ , otherwise it will cause unwanted losses in the rotor performance; and the twist adjustment step is set equal to  $5^\circ$ . The  $a_{twi}$  defining parameter is hence set in the following linear way:

$$a_{twj} = \frac{b_{up}-b_{twi}j}{r_{end}-r_0}j \quad (5)$$

where  $j$  varies from 0 to 1 with a step of 0.5. The values are based on designer assumptions and influence the density of functions family only.

### Cross-sectional variation

For the search of the optimal case, different cross sections are considered. Currently their number is limited to fifteen cross sections of Sxxx, NACA6xxxx and FX66S1xxxx families frequently used in the wind turbine design. Information for profile unit coordinates and lift-drag characteristics can be found from Bertagnolio et al. (2001), Malcolm et al. (2002) and different web resources.

## RESULTS OF BEM BASED BLADE GEOMETRY IMPROVEMENT

The iterative procedure draws various combinations of blade efficiencies versus blade costs. Each combination introduces its own blade geometry. First, we investigated the optimal chord and twist distribution and left the cross sections untouched. With the above stated assumptions about iterative parameters, the total of 5293 cases were considered. The results for the power efficiency versus rotor cost including the original blade case are shown in Figure 7. It is interesting from the economic perspective, that small chord and twist adjustments may provide significant technical efficiency advantages.

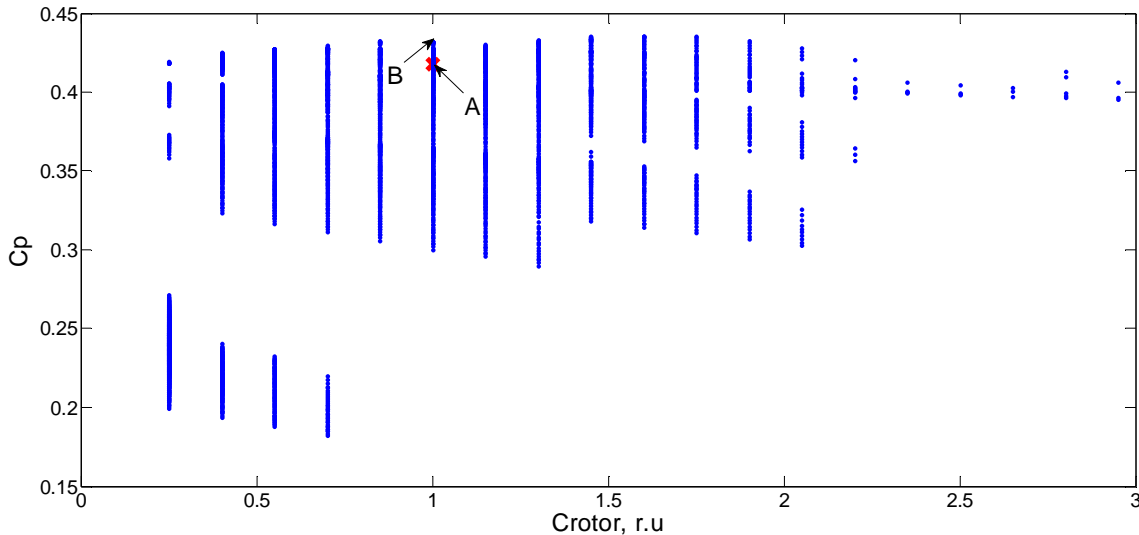


**Figure 7. Power coefficient versus rotor cost for different chord and twist distributions**

Cases A and B present the initial and modified cases for the maximum power coefficient and same rotor cost blade shapes. Investigations show that the original blade geometry has  $C_p=0.418$ , and with the modified chord and twist distributions, the respective coefficient can be raised up to 0.432. Improvement in the performance efficiency for 2% is considered as a great advantage.

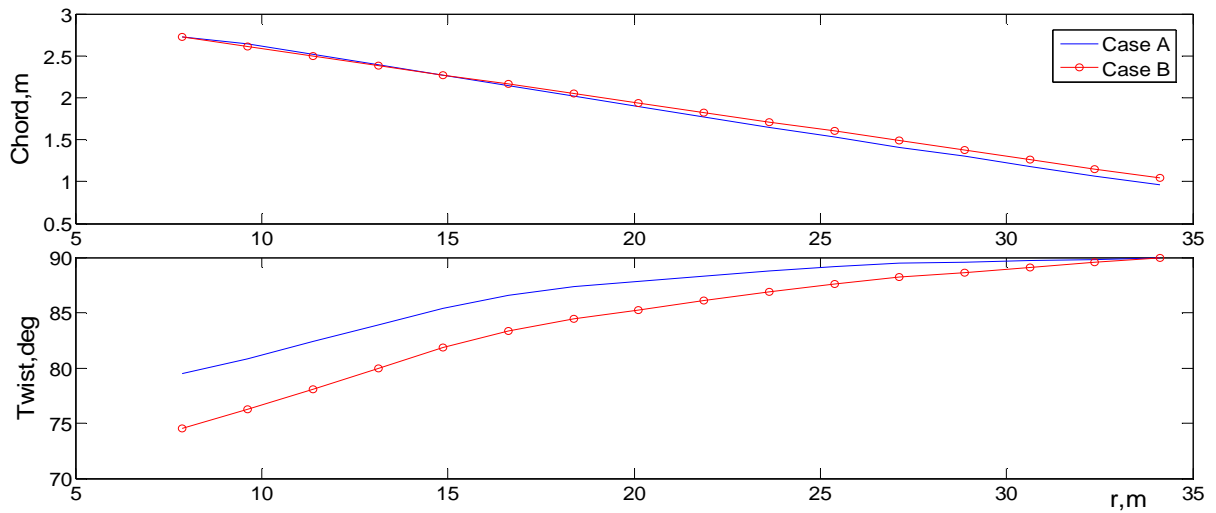


Figure 8. Chord and twist distributions for cases A and B

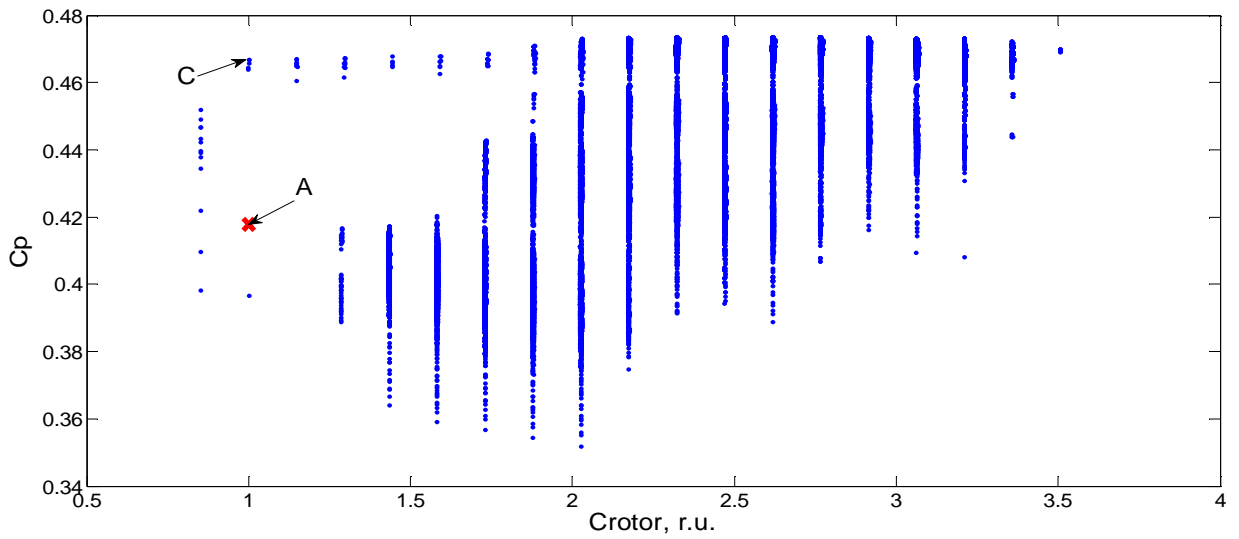
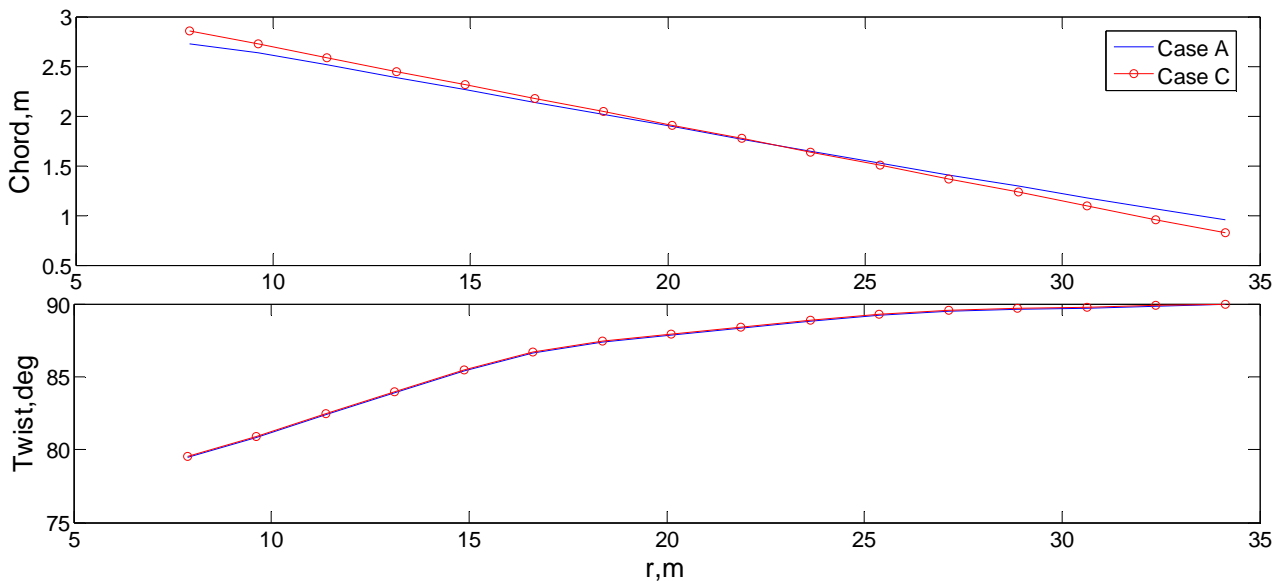


Figure 9. Power coefficient versus rotor cost for different chord, twist and cross-sectional distributions



A:	S818	S818	S818	S818	S818	S825	S826	S826	S826							
C:	NACA65421	S818	S818	S818	S818	S825	S826	S826	S826							

Figure 10. Chord, twist and cross-sectional distributions for cases A and C

Chord and twist distributions for the initial and optimal cases A and B are shown in Figure 8.

Next, the possibility for the cross-section variation is added. The number of considered cases equated to 36000. The respective results for the power efficiency versus rotor cost are shown on Figure 9. A significant improvement in the power efficiency can be obtained with the introduction of better suited airfoil and at the same time with relatively constant expenses. Cases A and C show the initial and modified cases for the maximum efficiency and same rotor cost. The respective chord, twist and cross-sectional variations are presented in Figure 10.

The blade shape C is the local maximum in the stated problem of optimal case search. The analyzed power coefficient for case C equals to  $C_p=0.467$ . Compared to the original blade geometry, it is considered as a significant improvement.

Now when the three cases, A, B and C, as the most interesting ones, are found, we proceed with CFD results validation.

### VALIDATION OF RESULTS WITH CFD-RANS COMPUTATIONS

The mathematical governing equations describing the aerodynamics of wind turbines are based on the equations of conservation of the momentum, mass and energy. The governing equations for the compressible Newtonian fluid are named as Navier-Stokes (NS) equations. The fluid is considered as incompressible and a RANS approach based on empirical  $k-\omega$  SST was used to model turbulence. This approach is based on the transport equations for the turbulence kinetic energy  $k$  and the specific dissipation rate  $\omega$ . According to IIIB IEC wind turbine class referred in this study, the turbulence parameters for the intensity and length scale equate to 16% and 150 m, respectively.

#### Mesh generation

The commercial software is used to build a computational domain and hexahedral meshes of approximately 2.5 million elements. The computational domain is conically shaped, and extends in the y-direction for 5 diameters upstream and 10 diameters downstream of the rotor. These dimensions have been chosen as a result of dedicated study on outer boundaries dependency according to Carcangiu (2008).

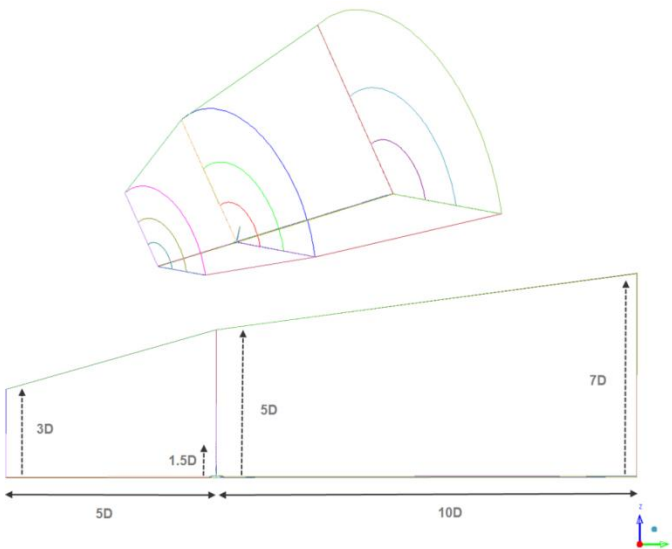


Figure 11. Computational domain

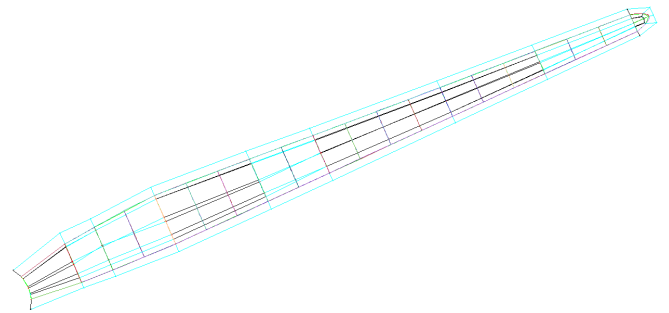
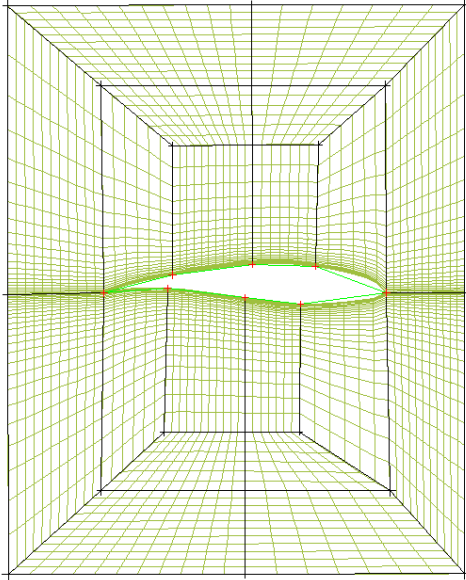


Figure 12. 3D block topology model around the blade

The tower and the ground are not included in the model. To generate the volume mesh around the three blade rotor, the 120 degrees periodicity of the rotor is used, by meshing only the volume around one blade. The other two blades are included in the computations using periodic boundary conditions.

Block topology approach was used during the mesh generation process. After creating a 3D block topology model equivalent to the geometry, the block topology was further refined through the splitting of edges, faces and blocks. To ensure good quality of the mesh body-fitted internal and external O-grids was generated to parametrically fit the block topology to the geometry. The mesh resolution was refined in the proximity of the blade and rotor sections in order to obtain  $y^+$  around 5.



**Figure 13. O-grid around the blade section (axi-radial plane).**

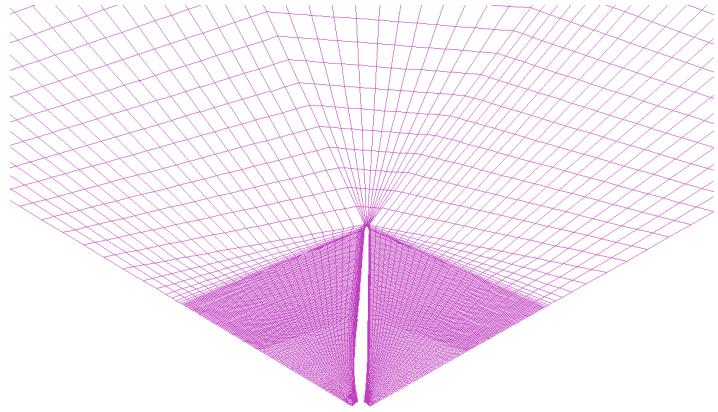


**Figure 14. Mesh around the blade section (meridional plane).**

To provide accurate results, the dependence of the power coefficient on the grid size is investigated. The initial blade geometry is taken for the grid sensitivity analysis. The coarse meshes consist of  $0.64 \cdot 10^6$  and  $1.43 \cdot 10^6$  elements; the fine mesh considers  $2.58 \cdot 10^6$  elements; and the refined mesh -  $3.22 \cdot 10^6$ .

Results of the grid sensitivity analysis, presented on Figure 15, show that the fine mesh of  $2.58 \cdot 10^6$  elements provides enough accurate results and can be used for further calculations.

Results of CFD-RANS computations

The commercial CFD solver is used for the full 3D RANS wind turbine rotor computations. All simulations are performed assuming a steady state condition within a moving reference frame.

Uniform wind velocity  $U = 7.5$  m/s is set at the inlet and at lateral faces, and a pressure outlet condition is placed at the outlet. No-slip condition is assumed for the surface of the blades and the nacelle. The generator housing rotates at a fixed rotational speed 1.47 rad/s together with the blades,

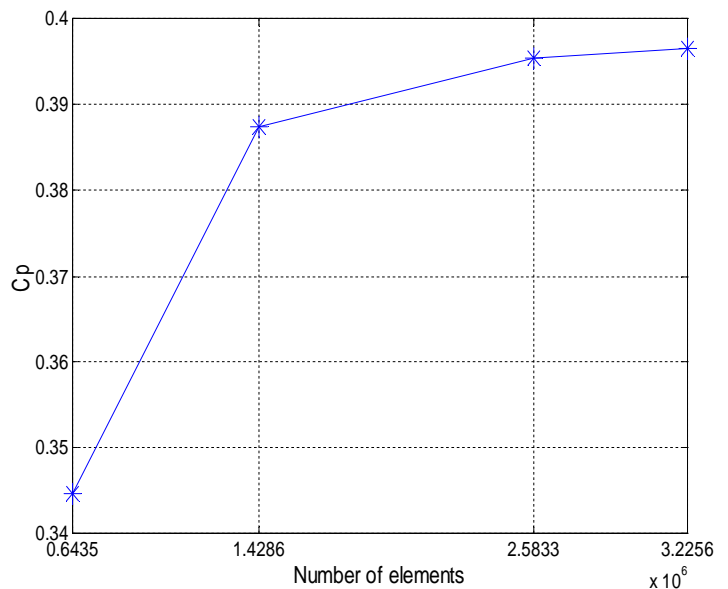


**Figure 15. Dependence of power coefficient on the grid size.**

in contrast to the real applications where only a small portion (hub) rotates. In our case, where hub is axisymmetric, this allowed keeping the model simple.

The results for three considered blade geometries, cases A, B, and C, are presented as power coefficients. CFD and BEM based values of aerodynamic power efficiency are compared in Table 1.

**Table 1. Comparable power coefficient results for CFD and BEM calculations.**

	<b>Case A</b>	<b>Case B</b>	<b>Case C</b>
<b>BEM</b>	0.418	0.432	0.467
<b>CFD-RANS</b>	0.395	0.418	0.44

The results correlate with the overall trend, and the minor fluctuations are discussed in conclusions.

## CONCLUSIONS

This work develops an iterative semi-automated search mechanism for wind blade geometry improvement. The rapid wind industry growth shows a clear demand for such a tool. The implementation of the lately introduced aerodynamic, economic and mechanic analysis technique coupled with robust airfoil characteristics coding allowed to fasten the search procedure and to use the extensively applied Matlab programming environment. The obtained modified solutions based on the power efficiency improvement while maintaining the same capital investments as the original blade geometry, provided significant advantages. While looking for the optimal chord and twist distribution for the considered WindPACT 1.5 MW wind turbine and IIIB IEC wind class with the BEM approach, the power efficiency was improved by 1.4% compared to the original blade geometry. The same procedure coupled with the optimal cross-sectional search provided an improvement of 4.9% in the power coefficient. The results were validated against the CFD procedure. Three variants were considered: the original shape; the modified distribution for chord and twist; and the modified distribution for chord, twist and cross-section. The difference in the BEM and CFD calculations are explained with empirical and hence semi-accurate characterization of the airfoil lift and drag curves introduced in the article. Moreover, the turbulence of the  $k-\omega$  SST model in the CFD-RANS procedure takes into account the turbulent properties of the flow which are not considered in the BEM technique.

The work showed an adequate applicability of the proposed semi-automated improvement approach. The future work is aimed for further airfoils database expansion and visualization of pre and post processing.

## ACKNOWLEDGEMENTS

This research work was done within the RENEWTECH project funded by the European Regional Development Fund (ERDF).

## References

- Evans P., (2012), *Wind growth rests on non-OECD demand: GWEC. Wind market report*, Renewable energy world magazine, vol.15/3, pp.14-16
- Casas V.D., Pena F.L., Duro R.J., (2006), *Automatic design and optimization of wind turbine blades*, International Conference on Computational Intelligence for Modeling Control and Automation
- Fuglsang P. Madsen H.A., (1999), *Optimization method for wind turbine rotors*, Journal of Wind Engineering and Industrial Aerodynamics, 80, pp.191-206
- Lyytikäinen M., Hämäläinen T., Hämäläinen J., (2009), *A fast modelling tool for plate heat exchangers based on depth-averaged equations*, International Journal of Heat and Mass Transfer, 52, pp. 1132-1137

- Toivanen J., Hämäläinen J., Miettinen K., Tarvainen P., (2003), *Designing Paper Machine Headbox Using GA*, Materials and Manufacturing Processes, 18/3, pp. 533-541
- Ingram G., (2011), *Wind turbine blade analysis using the Blade Element Momentum Method*, [http://www.dur.ac.uk/g.l.ingram/download/wind\\_turbine\\_design.pdf](http://www.dur.ac.uk/g.l.ingram/download/wind_turbine_design.pdf) (accessed 20/11/2011)
- Moriarty P.J., Hansen A.C., (2005), *AeroDyn Theory Manual*, Technical report.
- Madsen H.A., Bak C., Døssing M., Mikkelsen R., Øye S., (2010), *Validation and modification of the Blade Element momentum theory based on comparisons with actuator disc simulations*, Wind Energy, Vol. 13, pp. 373-389.
- IEC 61400-12-1 1st ed., (2005), *Wind turbines – Part 12-1: Power Performance Measurements of Electricity Producing Wind Turbines*, International Electrotechnical Committee.
- Merz K.O., (2011), *Conceptual design of a stall regulated rotor for a deepwater offshore wind turbine*, Doctoral Thesis, Norwegian University of Science and Technology (NTNU), pp.31-35.
- Bir G., Migliore P., (2004), *Preliminary structural design of composite blades for two and three-bladed rotors*, Technical report.
- Tong W., (2010), *Wind power generation and wind turbine design*, WIT Press, p. 210.
- Malcolm D.J., Hansen A.C., (2002), *WindPACT turbine rotor design study*, Subcontractor report.
- Xudong W. et al., (2009), *Shape optimization of wind turbine blades*, Wind Energy, Vol. 12, No. 8, pp. 781-803.
- Perfiliev D., (2011), *Optimization of wind blade design including its energetic characteristics*, LAP Lambert Academic Publishing, pp. 35-41
- Bertagnolio F., Sorensen N., Johansen J., Fuglsang P., (2001), *Wind turbine airfoil catalogue*, Riso National Laboratory, Roskilde, Denmark
- Rajendran C., (2011), *Techniques for enhancing wing energy generation – a CFD based multibody dynamics approach in horizontal axis wind turbines*, Doctoral Thesis, Cochin University of Science and Technology
- Chao D.D., van Dam C.P., (2008), *CFD Analysis of Rotating Two-Bladed Flatback Wind Turbine Rotor*, Sandia report, Sandia National Laboratories
- Hansen M.O.L., Sorensen N.N., Sorensen J.N., Michelsen J.A., (1997), *Extraction of lift, drag and angle of attack from computed 3-D viscous flow around a rotating blade*, In Proceedings of EWEC 97: Dublin, vol. 13, pp. 499–502
- Carcangiu C.E., (2008), *CFD-RANS Study of Horizontal Axis Wind Turbines*, Doctoral Thesis, Università degli Studi di Cagliari.
- Cao H., (2011), *Aerodynamics Analysis of Small Horizontal Axis Wind Turbine Blades by Using 2D and 3D CFD Modelling*, Master thesis, University of the Central Lancashire.
- Shives M.R., (2008), *Hydrodynamic Modeling, Optimization and Performance Assessment for Ducted and Non-ducted Tidal Turbines*, Master's thesis, University of Victoria
- Hansen M.O.L., Sorensen J.N., Voutsinas S., Sørensen N., Madsen H. Aa., (2006), *State of the art in wind turbine aerodynamics and aeroelasticity*, Progress in Aerospace Sciences.
- Vermeer L.J., Sorensen J.N., Crespo A., (2003), *Wind turbine wake aerodynamics*, Progress in Aerospace Sciences.